Ionization Energies of Niobium Carbide Clusters Nb_nC_m ($n = 3-10$, $m = 0-7$)

Naoya Fukushima, Ken Miyajima, and Fumitaka Mafuné*

Department of Basic Science, Graduate School of Arts and Sciences, The University of Tokyo, Komaba, Meguro-ku, Tokyo 153-8902, Japan

Received: November 10, 2008; Revised Manuscript Received: December 25, 2008

We prepared niobium carbide clusters, Nb_nC_m, in the gas phase by a double laser ablation technique. A photoionization efficiency was measured as a function of the wavelength of an ionization laser to determine ionization energies (E_i's) of Nb_nC_m ($n = 3-10$, $m = 0-7$). The E_i's of Nb_4C_4 and Nb_5C_3 are found to be the lowest in the clusters studied. When the experimental E_i's are compared with the E_i's estimated by the density functional calculation previously reported (Harris, H.; Dance, I. *J. Phys. Chem. A* 2001, *105*, 3340−3358), we determined Nb_5C_3 to have a similar $2 \times 2 \times 2$ cubic structure as Nb_4C_4. We also found that the E_i's of carbon-rich clusters, Nb_nC_m ($n \leq m$), tend to be higher (>5 eV) than the E_i's of the niobium-rich clusters. The high E_i's are due to the structure of the carbon-rich clusters: carbon−carbon bonding is preferred when the number of carbon atoms exceeds the number of metal atoms. The structure was also discussed in relation to the reactivity of cluster ions with a hydrogen molecule.

Introduction

Since the first report of metallocarbohedrene, Ti_8C_{12}, in 1992, a variety of types of metal carbide clusters have been investigated.[1−7] For niobium carbide clusters, Nb_nC_m, cubic crystallites (e.g., Nb_4C_4) have been studied as intensively as metallocarbohedrenes (Nb_8C_{12}, $Nb_{13}C_{22}$).[7−15] For instance, Pilgrim et al. found that $Nb_4C_4^+$ is the dominant photodissociation product of larger cluster ions, suggesting enhanced stability of $Nb_4C_4^+$.[8] They proposed the geometrical structure of Nb_4C_4 to be a $2 \times 2 \times 2$ cube. Yeh et al. studied reactivity of $Nb_4C_4^+$ with a range of molecules including oxygen, water, methanol, etc.[12] They calculated the structure of Nb_4C_4 to understand the reactivity and showed that Nb_4C_4 has the $2 \times 2 \times 2$ cubic structure. van Heijnsbergen et al. obtained the infrared resonance-enhanced multiphoton ionization (IR-REMPI) spectrum of Nb_4C_4 using the FELIX tunable infrared-free electron laser.[15] They observed a broad absorption band at 675 cm^{-1}, which was assigned to the IR-active phonon mode of the metallic NbC(100) surface, giving the direct evidence for the $2 \times 2 \times 2$ cubic structure.

Other small niobium carbide clusters have also been investigated. Yang et al. obtained pulsed field ionization zero electron kinetic energy (PFI-ZEKE) photoelectron spectrum of Nb_3C_2.[16] The spectrum shows a long vibronic progression, suggesting that the cluster has a trigonal bipyramid structure. For NbC_n^+, Clemmer and Jarrold investigated the geometrical structure of carbon units by ion mobility measurements.[17] As a result, isomers containing monocyclic and bicyclic rings, graphitic sheets, and mettalofullerences have been identified. More recently, Dryza et al. measured the ionization energies (E_i's) of Nb_3C_m ($m = 1-4$) and Nb_4C_m ($m = 1-6$). They determined the geometrical structures of the small clusters by comparing the experimental E_i's with the calculated ones.[18]

As exemplified above, niobium carbide clusters which have been investigated so far are mostly limited to small Nb_nC_m clusters ($n + m < 8$) or large Nb_nC_m clusters with $1 \leq m/n \leq 1.5$ ($n \leq 9$). In fact, Harris and Dance have systematically calculated 100 isomers of 28 different Nb_nC_m clusters by the density functional theory (DFT), ranging within $m/n \sim 1$.[19] It is probably because the clusters were formed in a pulsed laser ablation source in the presence of hydrocarbons in most cases, and clusters with $m/n \sim 1$ tend to be formed abundantly.

In the present study, we used a double laser ablation source, where the niobium and carbon vapor were produced by the laser pulses in the gas phase, then coaggregating to form clusters. This double laser ablation source enables us to prepare a variety of multielement clusters such as Nb_nC_m over the wide size and stoichiometry ranges. In fact, we examined hydrogen attachment reaction of $Nb_nC_m^+$ ($1 \leq n \leq 9$, $0 \leq m \leq 16$) in the previous study.[20] We found the general trend of the cluster composition dependence that carbon-rich cluster ions are less reactive than the niobium-rich cluster ions.

Here, we measured photoionization efficiency spectra for Nb_nC_m ($3 \leq n \leq 10$, $0 \leq m \leq 7$), from which E_i's were obtained. By overviewing a map of the E_i's, we found that the E_i's of carbon-rich clusters are higher than those of the other clusters. This trend could relate to the reactivity of $Nb_nC_m^+$ with H_2. Furthermore, we found that Nb_4C_4 and Nb_5C_3 are the lowest in the E_i in the clusters studied. The geometrical structure of them is discussed on the basis of the density functional calculation previously reported.

Experimental Section

Figure 1 shows an experimental setup used in the present study. Niobium carbide clusters were formed in a supersonic double laser ablation source coupled to a reflectron-equipped time-of-flight mass spectrometer. A niobium metal rod (99.9%) and a graphite rod (99.99%) were set downstream of the supersonic source from a solenoid pulsed valve (General Valve). Both rods (5 mm in diameter) were kept rotating and sliding inside a stainless block to maintain the stable laser ablation condition. The rods were irradiated with the focused laser pulses (~10 mJ/pulse) at a wavelength of 532 nm from Quanta Ray GCR-170 and Continuum Surelite II Nd^{3+}:YAG lasers for generating the plasma. The evaporated niobium and carbon were cooled in a waiting room (6 mm in diameter) by the He gas

* Corresponding author. E-mail: mafune@cluster.c.u-tokyo.ac.jp.

10.1021/jp809915c CCC: $40.75
Published on Web 02/18/2009

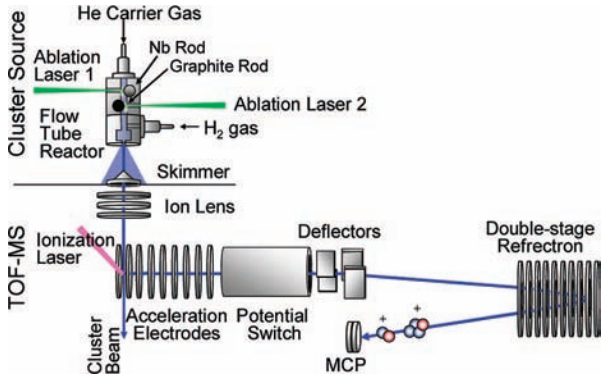

Figure 1. Experimental setup used in the present study.

(>99.99995%; 9 atm) from the valve, forming neutral and charged Nb_nC_m. The clusters were passed along a 2 mm in diameter and 60 mm long condensation tube before expansion into the first vacuum chamber and were introduced into the differentially pumped second chamber through a skimmer. The experiment was operated at 10 Hz. Timings of the laser pulses and the valve was controlled by Stanford DG535 delay generators so as for Nb_nC_m to form stably and abundantly. When the cluster ions $Nb_nC_m^+$ were monitored, the ions were accelerated orthogonally by the pulsed electric field for the time-of-flight mass analysis after they entered between a repeller and a first electrode (see Supporting Information Figure S2). When the neutral clusters were examined, the charged cluster ions were removed from the beam by the electric field applied to the electric lens equipped between the skimmer and the acceleration electrodes. The selected neutral clusters were ionized in the acceleration region with the frequency-doubled output of a Nd^{3+}:YAG-pumped OPO laser (Continuum Panther EX). The wavelength of the ionization laser was varied at the interval of 2 nm from 282 to 212 nm and additionally at 211 nm. The laser was collimated to a 6 mm diameter beam, and typical laser pulse energies used for photoionization were kept at 120 μJ as measured using a power meter (Coherent J-10MB-LE) to avoid extensive multiphoton ionization.

The ions, either the native or photoionized, gained the kinetic energy of ~3.4 keV in the acceleration region. As the voltage of the end electrode of the acceleration region is floated to −3.2 kV, we used a 304 mm long potential switch right after the end electrode to shift the voltage around the ions from −3.2 kV to zero. The voltage was switched by the Behlke HTS-50 high-voltage MOSFET. After the potential switch, the ions were steered and focused by a set of vertical and horizontal deflectors and an einzel lens. After traveling in a 1 m field-free region, the ions were reversed by the reflectron and were detected by a Hamamatsu double-microchannel plate detector. Signals from the detector were amplified by a Stanford SR445A 350 MHz preamplifier and processed by a Tektronix TDS 500A digital oscilloscope. Typically 200 spectra were averaged at each wavelength, which minimizes practically the short-term fluctuation. During the measurement of photoionization efficiency spectra, the abundance of native ions was monitored every 18 measurements in order to check the long-term fluctuation. The mass resolution, $m/\Delta m$, exceeds 1000.

Results

As mentioned above, neutral and charged Nb_nC_m were simultaneously formed in the gas phase by the double laser ablation source. Although the niobium metal rod was located 8 mm upstream from the graphite rod in our experimental setup, niobium and carbon vapor formed by the laser ablation were totally mixed together in the gas phase. We confirmed that the essentially same mass spectrum was obtained when the position of the two rods was exchanged. We have already reported the mass spectrum of positively charged native niobium carbide clusters in the previous study.[20] The cluster ions with $3x$ (x = 1, 2, 3) carbon atoms attached, $Nb_nC_{3x}^+$ are more abundant in the spectrum (see Supporting Information Figure S2). As the E_i's of Nb_nC_3 are lower than those of the other clusters, they could be ionized more readily in the plasma in the double laser ablation source. However, we do not consider the low E_i's as the most influential factors on the observed distribution of $Nb_nC_m^+$. Instead, the high abundance of $Nb_nC_3^+$ must be due to the high abundance of the neutral Nb_nC_3 in the gas phase. This conjecture is supported by the fact that, first, $Nb_nC_3^+$ are abundantly formed when the neutral clusters are ionized by the both single- and multiphoton ionization (250 nm; ~1.4 mJ/pulse) (see Supporting Information Figure S3). Under the condition, the ionization efficiency should not depend significantly on the stoichiometry. Second, when the clusters were ionized by the single photon, the signal intensity for Nb_5C_3 at 0.5 eV above the ionization threshold in the photoionization efficiency spectrum was 1 order of magnitude higher than that of Nb_5C_2 at similarly 0.5 eV above its threshold. Note that the ion signals mostly level off at 0.5 eV above the ionization threshold. Consequently, we can consider that the neutral Nb_nC_3 are also abundantly formed in the gas phase. Furthermore, it has been well-known that C_3 is a stable neutral fragment in the decomposition of small carbon clusters. Recently, a vacuum UV (VUV) photoionization mass spectrometry study by Belau et al. directly indicated that the neutral carbon vapor by laser vaporization contains more C_3 than C_2, and the density of C_3 is quite high compared to that of other carbon clusters.[21] Therefore, it is quite likely that high abundance of C_3 in the cluster formation region is the reason why high abundance of the $Nb_nC_{3x}^{0/+}$ was observed in this study.

In contrast, neutral and cationic Nb_nC_3 clusters are not prominent when they are formed by the gas-phase dehydrogenation reaction of acetylene or ethylene with the niobium clusters.[7−12,22] It should be noted that as far as we know there are two reports on the production Met-Car without hydrocarbon gases. Castleman's group used a mixture of metal−carbon powder, and Wang's group used TiC target. However, the enhancement of Ti_nC_3 clusters were not mentioned.[23,24]

Figure 2 shows the mass spectrum of niobium carbide clusters following laser photoionization at different wavelengths from 282 to 211 nm under otherwise identical conditions. In the spectrum recorded at 211 nm, many $Nb_nC_m^+$ clusters with specific combinations of (n, m) appear, suggesting that the mixed neutral clusters were evidently formed and ionized by the absorption of a photon at 5.88 eV. As the wavelength of the ionization laser increases, the peak intensity of each ion decreases differently. For instance, the peak intensity of $Nb_6C_3^+$ starts to decrease from 242 nm, which is totally reduced to the baseline level at 266 nm. By contrast to $Nb_6C_3^+$, the peak intensity of $Nb_5C_3^+$ does not change until 266 nm. The spectrum recorded at 274 nm exhibits that the intensity of all species has decreased to near baseline levels On the other hand, the small peaks of the Nb_5^+, $Nb_5C_3^+$, Nb_6^+, Nb_6C^+, Nb_7^+, and Nb_8^+ cluster ions are still observed at 278 nm. However, they are considered to be formed by the multiphoton absorption, since the laser fluence dependence of the peak intensity is not linear at 278 nm (not shown). In fact, Cole and Liu observed long-lived excited states in niobium clusters and they observed intense

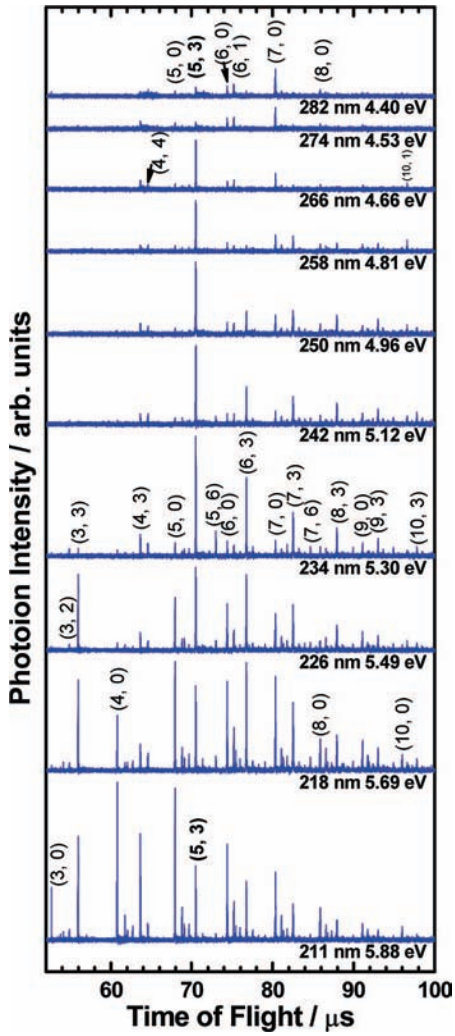

Figure 2. Mass spectrum of Nb_nC_m clusters following laser photoionization at different wavelengths from 282 to 211 nm. Laser fluence was kept at ~120 μJ/pulse. Wavelengths of the ionization laser and the assignment of the ion peaks are displayed.

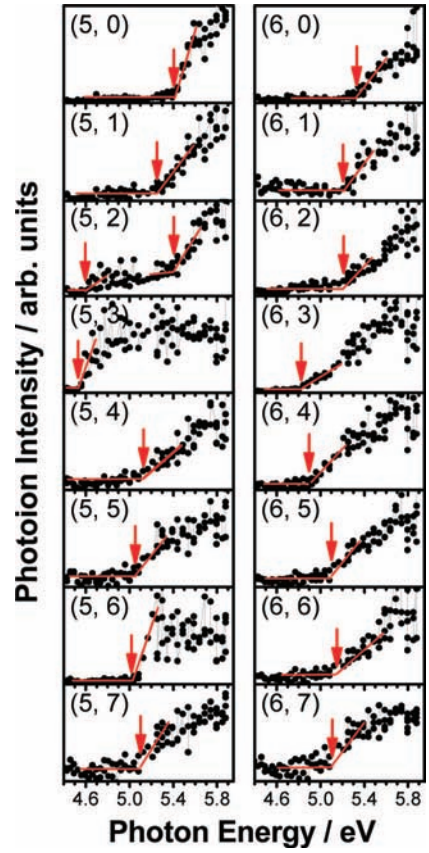

Figure 3. Photoionization efficiency spectra for Nb_5C_m and Nb_6C_m (m = 0−7) clusters. Arrows indicate the lowest and second lowest ionization thresholds.

signal of Nb_7 at $h\nu$ = 5 eV which is consistent with our observation (see Supporting Information Figures S1 and S3).[25,26] Hence, we assign the onset which lies at the higher photon energy as the threshold for one-photon ionization. It should be noted that carbon-rich clusters, Nb_nC_m (n, m) = (3, $m \geq 5$), (4, $m \geq 6$), (5−9, $m \geq 8$), and (10, $m \geq 7$), were not observed in this study. Although Nb_2C_{0-3} clusters were observed at 211 nm, we were not able to determine E_i's due to the low signal intensity.

In order to determine the ionization energy, the photoionization efficiency spectrum was obtained by measuring the ion intensity of each cluster as a function of the wavelength. Figure 3 shows the photoionization efficiency spectra for the Nb_5C_m and Nb_6C_m (m = 0−6) clusters. Generally, the ion intensity which is near baseline level at lower photon energy, rises sharply at a threshold energy. For instance, the spectrum for Nb_5C_3 exhibits that the ion intensity is as high as the baseline level at 4.4 eV, rises dramatically at 4.53 ± 0.05 eV, and levels off above it. We fitted the straight line to the rise of the ion intensity and determined the appearance energy from the intersection of the straight line with the baseline. Uncertainties in the E_i's were determined from the lowest and highest values deduced from the intersection positions between the baseline and the upper and lower side of data spread width on the slope region. We have determined the E_i's for a variety of the Nb_nC_m clusters and Nb_nO clusters in the present study (see Table 1).

Our results for Nb_n, Nb_nO (n = 3−10), Nb_3C_m, and Nb_4C_m are in good agreement with those previously reported within experimental errors.[16,18,19,25,27] However, the agreement is not trivial, because the niobium carbide clusters were prepared by the different methods: We prepared the clusters by the gas-phase aggregation of the niobium and the carbon vapor from the double laser ablation source, whereas in most cases, the niobium carbide clusters were prepared by the gas-phase dehydrogenation reaction of hydrocarbons with the niobium clusters. The agreement of the E_i's as well as the features of the photoionization efficiency spectra indicates that the same isomers were formed by the two different methods except for several clusters. This is reasonable, because isomers that were assigned as the most stable one by the density functional calculation were principally formed by both experiments except for several cases, which will be discussed later.

Figure 4 shows the determined E_i's for Nb_nC_m clusters as a map as functions of both the numbers of carbon atoms and niobium atoms. Some clusters exhibited double E_i onsets in the photoionization efficiency spectrum, which are displayed by a filled circle in the map. For example, the photoionization efficiency spectrum for Nb_4C_2 cluster has two onsets as shown in Supporting Information Figure S1, which have been observed by Dryza et al.[18] By overviewing the map, we noticed the trend that the niobium-rich clusters, Nb_nC_m ($n \leq m$, $m \geq 3$), exhibit lower E_i's (<5 eV), whereas carbon-rich clusters, Nb_nC_m ($n \leq m$), show higher E_i's (>5 eV). In addition, E_i's of Nb_nC_3 are slightly lower than those of the other clusters.

TABLE 1: List of Experimental E_i's (eV) Observed for Nb_nC_m and Nb_nO (Also Listed are Calculated E_i's)

cluster	E_i (this work)	E_i (exptl)[a,b,c,d]	E_i (exptl)[e]	E_i (calcd)[c,e,f]
Nb_3	5.79 ± 0.06	5.81 ± 0.05[a]	5.79 ± 0.05	6.16[e]
Nb_3C_1	>5.88		>5.91	7.07[e]
Nb_3C_2	4.96 ± 0.06	5.046 ± 0.012[c]	5.02 ± 0.05	5.16[c], 5.58[e]
Nb_3C_3	5.31 ± 0.07		5.34 ± 0.05	6.09[e], 5.59[f]
Nb_3C_4	5.60 ± 0.10		5.65 ± 0.05	6.73[e], 6.85[f]
Nb_4	5.60 ± 0.06	5.64 ± 0.05[a], 5.60 ± 0.05[b]	5.60 ± 0.05	5.96[e]
Nb_4C_1	5.7 ± 0.1		5.76 ± 0.05	6.11[e]
Nb_4C_2	5.2 ± 0.15		5.24 ± 0.05	5.85[e]
	5.5 ± 0.1			
Nb_4C_3	4.6 ± 0.1		4.52 ± 0.05	5.05[e]
	5.72 ± 0.06		5.72 ± 0.05	6.01[e]
Nb_4C_4	4.5 ± 0.1	4.43[c]	4.43 ± 0.05	4.87[e], 5.12[f]
		>5.76[d]		
Nb_4C_5	4.75 ± 0.15		4.74 ± 0.05	6.41[e]
Nb_5	5.40 ± 0.06	5.45 ± 0.05[a], 5.44 ± 0.05[b]		
Nb_5C_1	5.25 ± 0.08			
Nb_5C_2	4.6 ± 0.15	4.59[c]		
	5.4 ± 0.15			
Nb_5C_3	4.53 ± 0.05			4.47[f]
Nb_5C_4	5.12 ± 0.12			
Nb_5C_5	5.05 ± 0.10			
Nb_5C_6	5.02 ± 0.08			6.89[f]
Nb_5C_7	5.10 ± 0.12			
Nb_6	5.33 ± 0.06	5.38 ± 0.05[a], 5.37 ± 0.05[b]		
Nb_6C_1	5.25 ± 0.07			
Nb_6C_2	5.21 ± 0.07			
Nb_6C_3	4.82 ± 0.06			
Nb_6C_4	4.9 ± 0.1			
Nb_6C_5	5.1 ± 0.1			
Nb_6C_6	5.15 ± 0.12			5.25[f]
Nb_6C_7	5.1 ± 0.12			
Nb_7	5.33 ± 0.06	5.35 ± 0.05[a], 5.34 ± 0.05[b]		
Nb_7C_1	5.20 ± 0.08			
Nb_7C_2	4.7 ± 0.1			
Nb_7C_3	4.70 ± 0.08			
Nb_7C_4	4.75 ± 0.07			
Nb_7C_5	4.70 ± 0.10			
Nb_7C_6	4.91 ± 0.07			
Nb_7C_7	5.1 ± 0.1			
Nb_8	5.5 ± 0.1	5.39 ± 0.05[b], 5.53 ± 0.05[a]		
Nb_8C_1	5.1 ± 0.1			
Nb_8C_2	4.95 ± 0.12			
Nb_8C_3	4.75 ± 0.08			
Nb_8C_4	4.8 ± 0.1			
Nb_8C_5	4.85 ± 0.15			
Nb_8C_6	4.9 ± 0.1			
Nb_8C_7	4.80 ± 0.15			
Nb_9	4.9 ± 0.1	4.92 ± 0.05[a], 4.88 ± 0.05[b]		
		5.20 ± 0.05[a]		
Nb_9C_1	4.8 ± 0.1			
Nb_9C_2	4.83 ± 0.12			
Nb_9C_3	4.72 ± 0.08			
Nb_9C_4	4.83 ± 0.08			
Nb_9C_5	4.82 ± 0.10			
Nb_9C_6	4.85 ± 0.12			
Nb_9C_7	4.88 ± 0.12			
Nb_{10}	5.42 ± 0.08	5.48 ± 0.05[a], 5.51 ± 0.05[b]		
$Nb_{10}C_1$	4.55 ± 0.06			
$Nb_{10}C_2$	4.85 ± 0.15			
$Nb_{10}C_3$	4.78 ± 0.09			
$Nb_{10}C_4$	4.8 ± 0.1			
$Nb_{10}C_5$	4.9 ± 0.1			
$Nb_{10}C_6$	4.8 ± 0.1			
Nb_3O	5.5 ± 0.1	5.51 ± 0.05[b]		
Nb_4O	5.5 ± 0.1	5.49 ± 0.05[b]		
Nb_5O	5.20 ± 0.05	5.25 ± 0.05[b]		
Nb_6O	5.5 ± 0.1	5.49 ± 0.05[b]		
Nb_7O	5.3 ± 0.1	5.37 ± 0.05[b]		
Nb_8O	5.14 ± 0.07	5.26 ± 0.05[b]		
Nb_9O	4.75 ± 0.10	4.72 ± 0.05[b]		
$Nb_{10}O$	5.1 ± 0.1	5.23 ± 0.05[b]		

[a] Ref 25. [b] Ref 27. [c] Ref 16. [d] Ref 9. [e] Ref 18. [f] Ref 19.

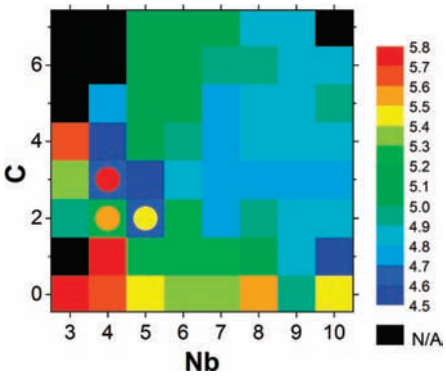

Figure 4. Map showing experimental values of E_i for Nb_nC_m clusters as a function of n and m. Each color corresponds to the E_i in eV, as indicated in the color code. Superimposed filled circles represent the energy of the second lowest E_i.

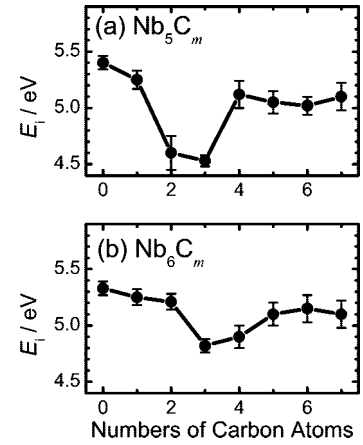

Figure 5. Graph showing experimental values of E_i for (a) Nb_5C_m clusters and (b) Nb_6C_m clusters as a function of m.

Discussion

Clusters of Low Ionization Energies. As shown in Figure 4 and Supporting Information Figure S1, we have determined the E_i's of about 70 clusters with different sizes and stoichiometries. E_i's of Nb_4C_4 and Nb_5C_3 were found to be the lowest in the niobium carbide clusters studied. Both clusters consist of eight atoms, and hence, they can form $2 \times 2 \times 2$ cubic structures.

For Nb_4C_4, we determined the E_i to be 4.5 ± 0.1 eV. This value is consistent with the experimental E_i of 4.43 ± 0.05 eV obtained by Dryza et al. within an experimental error.[18] Theoretical studies on Nb_4C_4 suggest that the most stable isomer has the $2 \times 2 \times 2$ cubic structure, where four C atoms are bound to the Nb faces of the tetrahedral Nb_4 cluster.[12,18,19] The E_i of Nb_4C_4 was calculated to be 4.87 and 5.12 eV, depending on the calculation method and the basis set. Hence, we assign the observed experimental E_i to $2 \times 2 \times 2$ cubic structure. Recently, Dryza et al. suggested that there are two close-lying singlet $^1A_1$ and triplet ^3B electronic states for the $2 \times 2 \times 2$ cube, being separated by only 0.067 eV.[18] They compared the IR-REMPI spectrum of Nb_4C_4 with the DFT-calculated IR spectra for the two spin states, concluding that Nb_4C_4 exists in the singlet state.

For Nb_5C_3, the E_i was determined to be 4.53 ± 0.05 eV. As far as we know, this is the first experimental data for the E_i of Nb_5C_3. It should be noted that in our experimental condition, Nb_5C_3 was the most abundantly observed $Nb_nC_{m>0}$ cluster by photon energy between 4.53 and 5.43 eV (see Figure 2). Harris and Dance calculated two isomers: one has a similar $2 \times 2 \times 2$ cubic structure as Nb_4C_4, one C atom is replaced by the Nb atom, and the other is a trigonal bipyramid of Nb atoms with a C atom between each pair of equatorial Nb atoms (D_{3h} symmetry).[19] The cubic structure was shown to be much more stable than the D_{3h} structure, and the E_i of the cubic structure was 4.47 eV. Hence, we assign the observed experimental E_i to the $2 \times 2 \times 2$ cubic structure.

The assignment is supported by the reactivity of $Nb_5C_3^+$ with a hydrogen molecule. In the previous study, we found that $Nb_5C_3^+$ reacts with a hydrogen molecule in a less extent, suggesting that the highest occupied molecular orbital−lowest unoccupied molecular orbital (HOMO−LUMO) gap of $Nb_5C_3^+$ is relatively larger.[20] The photoionization efficiency spectrum of Nb_5C_3 rises sharply from the baseline at the ionization threshold and levels off quickly after the linear rise, indicating good Franck−Condon overlap between the electronic states of the neutral and cation. Hence, the structure of the cation is close to the structure of the neutral, indicating that $Nb_5C_3^+$ also has the rigid $2 \times 2 \times 2$ cubic structure. The large HOMO−LUMO gap of the cation for the cubic structure (1.61 eV)[19] accords well with the low reactivity with the hydrogen molecule.[20] Note that the HOMO−LUMO gap for the D_{3h} structure is as low as 0.18 eV.[19]

Ionization Energies of Carbon-Rich Clusters. Figure 5 shows the determined E_i's of the Nb_5C_m and Nb_6C_m ($m = 0-7$) as a function of the numbers of carbon atoms. For the Nb_5C_m series, the E_i's of Nb_5C, Nb_5C_2, Nb_5C_3 are lower than the E_i of Nb_5, whereas the E_i turns to increase with the further addition of carbon atoms. In the Nb_6C_m series, the E_i's of Nb_6C_m ($m = 0-4$) are lower than the E_i of Nb_6; the E_i's increase with the further addition of carbon atoms. Similar V-shape changes are known for Nb_3C_m ($m = 0-4$) and Nb_4C_m ($m = 0-6$).[18]

In addition, the map in Figure 4 shows that the V-shape dependence is the general trend for the niobium carbide clusters over the wide size and stoichiometry ranges. In fact, carbon-rich clusters such as Nb_3C_4, Nb_4C_5, Nb_5C_6, and Nb_6C_7 are found to be higher in the E_i, when they are compared with the niobium-rich clusters such as Nb_6C_4, Nb_7C_5, Nb_8C_7, etc. (see Table 1 and Figure 4). We consider that the formation of a C_2 unit in the carbon-rich clusters induces the interaction between the niobium atoms and C_2, increasing the E_i's, because of the following reasons. First, it is well-known that a C_2 unit tends to be formed in the carbon-rich clusters: Dryza et al. discussed the development of the geometrical structures when the carbon atoms attach to Nb_3 and Nb_4 one by one.[18] From Nb_3C to Nb_3C_3, carbon atoms are bound to a face of the Nb_3 triangle and/or bound across the Nb−Nb edge. For Nb_3C_4, carbon atoms start to form a C_2 unit bound to the face of the Nb_3 triangle. Similarly, from Nb_4C to Nb_4C_4, carbon atoms bound to a face of the tetrahedral Nb_4. For Nb_4C_5, carbon atoms start to form a C_2 unit bound to the face of the tetrahedral Nb_4C_4. Recently Joswig and Springborg calculated structures and energies of Ti_nC_m clusters and discussed the influence of C_2 units on the stability of Ti_nC_m clusters. It was shown that the clusters containing C_2 dimers are energetically favored with respect to those containing only single carbon atoms or trimers.[28] Harris and Dance calculated the geometrical structure for larger niobium carbide clusters.[19] They showed that the most stable isomers for Nb_6C_7, Nb_6C_8, and Nb_7C_9 also involve the C_2 unit: Nb_6C_7 and Nb_6C_8 have one and three C_2 unit(s), respectively. Hence, carbon−carbon bonding is preferred when the number of carbon atoms exceeds the number of metal atoms. Second, the C_2 unit strongly interacts with the Nb atoms in the close vicinity. It is known that the

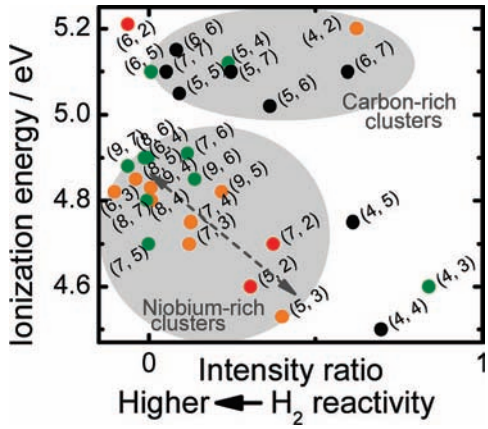

Figure 6. Correlation map between the ionization energy E_i of Nb_nC_m and relative reactivity defined as the ratio of the intensity of $Nb_nC_m^+$ after the reaction with H_2 to the ion intensity before the reaction (ref 20). The experimental error of relative reactivity is estimated as ~20%. The color of filled circles indicates the ratio of carbon atoms within the cluster: black, green, orange, and red are >50%, ~40%, ~30%, and <30%, respectively.

acetylide unit (C_2^{2-}) undergoes σ interaction and two side-on π interactions with the Nb atoms.[6] This electronic interaction is likely to stabilize neutral Nb_nC_m, increasing the E_i's of the carbon-rich clusters.

Reactivity with H_2. The carbon−carbon bonding is likely to reduce the reactivity of the cluster ions with a hydrogen molecule. In fact, according to our previous study, the reactivity is higher for the niobium-rich cluster ions, whereas the reactivity is lower for the carbon-rich cluster ions.[20] It is probably because the C_2 unit may occupy the active surface site of the niobium cluster ions.[28]

It could also be possible that the energetic balances influence the reactivity of $Nb_nC_m^+$. For the neutral Nb_n clusters, it is known that the size dependence of the reactivity with H_2 or N_2 correlates well with that of E_i: The reactivity decreases with an increase in E_i.[28−31] The strong correlation suggests that electron transfer from the neutral cluster to the hydrogen antibonding orbital is the rate-determining step in the reaction. Hence, as far as the cations are concerned, the HOMO−LUMO gap of $Nb_nC_m^+$ could correlate with the reactivities of $Nb_nC_m^+$ with H_2. However, there is no clear correlation between relative H_2 reactivity of $Nb_nC_m^+$ and the corresponding HOMO−LUMO gap values calculated by Harris and Dance.[19,20] Figure 6 shows the correlation map between the ionization energy of the Nb_nC_m clusters and reactivity of $Nb_nC_m^+$ defined as the ratio of the intensity of $Nb_nC_m^+$ after the reaction with H_2 to the ion intensity before the reaction. The map exhibits that there are two groups: the niobium-rich clusters are found in the lower E_i (<5 eV), whereas the carbon-rich clusters are found in the higher E_i (~5.1 eV), respectively. It is interesting to note that there may be a weak correlation between the ionization energy and the reactivity in each group: As the ionization energy increases, the reactivity also increases (as indicated by an arrow in the plot). However, there is no other indication on it by the experiments. For the further discussion, measurement of the reactivity for neutral Nb_nC_m with H_2 is required.

Conclusion

We prepared niobium carbide clusters, Nb_nC_m, in the gas phase by the double laser ablation technique. We measured a photoionization efficiency spectrum for Nb_nC_m, from which the E_i was obtained. By overviewing the map of E_i, the E_i's of Nb_4C_4 and Nb_5C_3 with $2 \times 2 \times 2$ cubic structure are found to be the lowest in the clusters studied. We also found that carbon-rich clusters, Nb_nC_m ($n \leq m$), have higher E_i compared to niobium-rich clusters. According to the theoretical works for metal−carbide clusters, the carbon-rich clusters tend to have C_2 units in them, which stabilize neutral Nb_nC_m by the interactions between the π electrons of C_2 and d orbitals of the Nb atoms. The conjecture is supported by our previous study on the reactivity of $Nb_nC_m^+$ with H_2.

The science of multielement clusters has not been fully established. These multielement clusters become more important and useful in various research fields and applications. However, the facts are that there are a large number of combinations on the constituent atoms (stoichiometries), and hence, insight of all these individual clusters cannot be examined promptly. In order to avoid the complexity, it is very important to utilize the concept of combinatorial chemistry for the first step: by overviewing the physical and chemical properties of the clusters, the general trend over the wide size and stoichiometry ranges can be acquired.

Acknowledgment. This work is supported by the Grant-in-Aid for Scientific Research (B) (No. 19350005) from the Ministry of Education, Culture, Sports, Science and Technology, Japan (MEXT) and by the Genesis Research Institute, Inc. for the cluster research. F.M. acknowledges Dr. Greg Metha and Professor Mark A. Buntine for helpful discussions on the experimental setup.

Supporting Information Available: Photoionization efficiency spectra for Nb_nC_m and Nb_nO ($n = 3-10$; $m = 0-7$) clusters, mass spectrum of native $Nb_nC_m^+$ cluster ions produced in the double laser ablation source, and mass spectrum of Nb_nC_m clusters photoionized at 250 nm. This material is available free of charge via the Internet at http://pubs.acs.org.

References and Notes

(1) Guo, B. C.; Kerns, K. P.; Castleman, A. W., Jr. *Science* **1992**, *255*, 1411–1413.
(2) Guo, B. C.; Wei, S.; Purnell, J.; Buzza, S.; Castleman, A. W., Jr. *Science* **1992**, *256*, 515–516.
(3) Wei, S.; Guo, B. C.; Purnell, J.; Buzza, S.; Castleman, A. W., Jr. *Science* **1992**, *256*, 818–820.
(4) Pilgrim, J. S.; Duncan, M. A. *J. Am. Chem. Soc.* **1993**, *115*, 9724–9727.
(5) Wei, S.; Castleman, A. W., Jr. *Chem. Phys. Lett.* **1994**, *227*, 305–311.
(6) Rohmer, M.-M.; Bénard, M.; Poblet, J. M. *Chem. Rev.* **2000**, *100*, 495–592.
(7) He, S.-G.; Xie, Y.; Dong, F.; Bernstein, E. R. *J. Chem. Phys.* **2006**, *125*, 164306.
(8) Pilgrim, J. S.; Brock, L. R.; Duncan, M. A. *J. Phys. Chem.* **1995**, *99*, 544–550.
(9) Brock, L. R.; Duncan, M. A. *J. Phys. Chem.* **1996**, *100*, 5654–5659.
(10) Purnell, J.; Wei, S.; Castleman, A. W., Jr. *Chem. Phys. Lett.* **1994**, *229*, 105–110.
(11) Wei, S.; Guo, B.; Deng, H.; Kerns, K.; Purnell, J.; Buzza, S.; Castleman, A. W., Jr. *J. Am. Chem. Soc.* **1994**, *116*, 4475–4476.
(12) Yeh, C. S.; Byun, Y. G.; Afzaal, S.; Kan, S. Z.; Lee, S.; Freiser, B. S.; Hay, P. J. *J. Am. Chem. Soc.* **1995**, *117*, 4042–4048.
(13) Byun, Y. G.; Kan, S. Z.; Lee, S. A.; Kim, Y. H.; Miletic, M.; Bleil, R. E.; Kais, S.; Freiser, B. S. *J. Phys. Chem.* **1996**, *100*, 6336–6341.
(14) Byun, Y. G.; Lee, S. A.; Kan, S. Z.; Freiser, B. S. *J. Phys. Chem.* **1996**, *100*, 14281–14288.
(15) van Heijnsbergen, D.; Fielicke, A.; Meijer, G.; von Helden, G. *Phys. Rev. Lett.* **2002**, *89*, 013401.
(16) Yang, D. S.; Zgierski, M. Z.; Bérces, A.; Hackett, P. A.; Roy, P.-N.; Martinez, A.; Carrington, T., Jr.; Salahub, D. R.; Fournier, R.; Pang, T.; Chen, C. *J. Chem. Phys.* **1996**, *105*, 10663–10671.
(17) Clemmer, D. E.; Jarrold, M. F. *J. Am. Chem. Soc.* **1995**, *117*, 8841–8850.

(18) Dryza, V.; Addicoat, M. A.; Gascooke, J. R.; Buntine, M. A.; Metha, G. F. *J. Phys. Chem. A* **2008**, *112*, 5582–5592.
(19) Harris, H.; Dance, I. *J. Phys. Chem. A* **2001**, *105*, 3340–3358.
(20) Miyajima, K.; Fukushima, N.; Mafuné, F. *J. Phys. Chem. A* **2008**, *112*, 5774–5776.
(21) Belau, L.; Wheeler, S. E.; Ticknor, B. W.; Ahmed, M.; Leone, S. R.; Allen, W. D.; Schaefer, H. F., III; Duncan, M. A. *J. Am. Chem. Soc.* **2007**, *129*, 10229–10243.
(22) Jiao, C. Q.; Freiser, B. S. *J. Phys. Chem.* **1995**, *99*, 10723–10730.
(23) Cartier, S. F.; May, B. D.; Castleman, A. W., Jr. *J. Phys. Chem.* **1996**, *100*, 8175–8179.
(24) Wang, L. S.; San Li, S.; Wu, H. *J. Phys. Chem.* **1996**, *100*, 19211–19214.
(25) Knickelbein, M. B.; Yang, S. *J. Chem. Phys.* **1990**, *93*, 5760–5767.
(26) Cole, S. K.; Liu, K. *J. Chem. Phys.* **1988**, *89*, 780–789.
(27) Athanassenas, K.; Kreisle, D.; Collings, B. A.; Rayner, D. M.; Hackett, P. A. *Chem. Phys. Lett.* **1993**, *213*, 105–110.
(28) Joswig, J.-O.; Springborg, M. *J. Chem. Phys.* **2008**, *129*, 134311.
(29) Whetten, R. L.; Zakin, M. R.; Cox, D. M.; Trevor, D. J.; Kaldor, A. *J. Chem. Phys.* **1986**, *85*, 1697–1698.
(30) Bérces, A.; Hackett, P. A.; Lian, L.; Mitchell, S. A.; Rayner, D. M. *J. Chem. Phys.* **1998**, *108*, 5476–5490.
(31) Knickelbein, M. B. *Annu. Rev. Phys. Chem.* **1999**, *50*, 79–115.

JP809915C